Fat Emulsification Measured Using NMR Transverse Relaxation

L. Marciani,* C. Ramanathan,*,[1] D. J. Tyler,* P. Young,* P. Manoj,† M. Wickham,† A. Fillery-Travis,†
R. C. Spiller,‡ and P. A. Gowland*,[2]

*Magnetic Resonance Centre, School of Physics and Astronomy, University of Nottingham, Nottingham NG7 2RD, United Kingdom; †Institute of Food Research, Colney, Norwich NR4 7UA, United Kingdom; and ‡Gastroenterology, Queen's Medical Centre, University Hospital, Nottingham NG7 2UH, United Kingdom

E-mail: penny.gowland@nottingham.ac.uk

This paper presents a novel method of measuring the droplet size in oil-in-water emulsions. It is based on changes in the NMR transverse relaxation rate due to the effect of microscopic magnetic susceptibility differences between fat droplets and the surrounding water. The longitudinal and transverse relaxation rates of a series of emulsions with constant oil volume fraction and five different mean droplet sizes, in the range 0.4–20.9 μm, were measured *in vitro* at 37°C using EPI. While the longitudinal relaxation rate $1/T_1$ did not change significantly, $1/T_2$ was observed to increase with mean droplet size. The measured changes in $1/T_2$ were found to be in good agreement with results predicted from proton random walk simulations, and were also consistent with analytical solutions based on an outer sphere relaxation model. Measurements of $1/T_2$ on emulsions with a higher oil volume fraction, and on emulsions of a fixed size where the water phase was doped with gadolinium to modulate the susceptibility difference between the phases, also showed the predicted behavior. As part of this study the susceptibility difference between olive oil and water was measured to be 1.55 ppm. © 2001 Academic Press

Key Words: relaxation rate, susceptibility, olive oil, emulsion, droplet size.

INTRODUCTION

Emulsion droplet size is an important parameter in food science and nutrition as well as in many other fields. It is usually measured using optical diffraction techniques (*1*). Diffusion-sensitive NMR measurements have also been used extensively to measure droplet size distributions (*2–7*), and NMR "diffusive-diffraction" effects have been observed in the emulsion diffusion curves (*8*). However, the pulsed gradient spin-echo sequence used in these experiments requires particularly high gradient amplitudes in order to provide adequate sensitivity.

It is known that NMR transverse relaxation times, measured using single-spin-echo experiments, are affected by diffusion in field gradients. This is why true T_2 relaxation times are measured

using CPMG multiecho experiments. In this paper we use T_2 to represent a transverse relaxation time that includes the effects of diffusion through magnetic field inhomogeneities. In particular, the value of T_2 measured in single-spin-echo experiments will depend on the size and distribution of any microscopic susceptibility perturber that gives rise to magnetic field gradients (*9–11*). It should therefore be possible to determine oil droplet size in emulsions using spin-echo measurements. Previous work on the relaxation times of emulsions has been aimed at measuring the magnitude of the oil fraction using T_1 (*12–14*).

This paper describes the measurement of the size of oil droplets in emulsions using EPI T_2 relaxometry. The difference in magnetic susceptibility between olive oil and water has been determined. The transverse relaxation rates of two different sets of emulsions with varying oil droplet sizes have been determined. The results are compared with an analytical model and Monte Carlo random walk simulations.

THEORY

This section describes the expected signal loss in a spin-echo sequence due to the susceptibility difference between spherical oil droplets and the surrounding water in oil-in-water emulsions. The signal changes due to microscopic susceptibility variations are quite complex (*9, 11, 15*), and general analytical solutions do not currently exist. However, analytical solutions can be obtained in the two limiting regimes of motional narrowing and static dephasing. These regimes can be defined in terms of the correlation time for diffusion with respect to the magnetic field inhomogeneities, $\tau_R = R^2/D$ (R is the radius of the susceptibility perturber, D is the diffusion coefficient of water), and the local Larmor frequency shift produced by the susceptibility differences, $\delta\omega$. The motionally narrowed regime, defined by $\delta\omega \cdot \tau_R \ll 1$, is usually valid for small perturbers or rapid diffusion. In this regime the protons sample the entire range of frequencies present in the sample (*16, 17*). It has been described analytically using outer sphere relaxation theory, originally derived for relaxation due to paramagnetic complexes (*18*). In the static dephasing regime, usually valid for large

perturbers or slow diffusion, $\delta\omega \cdot \tau_R \gg 1$, the effects of diffusion are small and the signal is largely refocused in a spin-echo experiment (19). We focus here on the motionally narrowed regime.

Gillis and Koenig have shown that the change in transverse relaxation rate ΔR_2 due to particulate susceptibility perturbations can be expressed as (17)

$$\Delta R_2 = \left(\frac{1}{T_2}\right)_{\text{emulsion}} - \left(\frac{1}{T_2}\right)_{\text{water}} = \frac{16}{135} f \left(\frac{\gamma \Delta\chi B_0}{3}\right)^2 \frac{R^2}{D},$$
[1]

where f is the volume fraction of the oil, γ the proton gyromagnetic ratio, $\Delta\chi$ the difference in magnetic susceptibility between oil and water, and B_0 the main static field (all in SI units). Thus at constant volume fraction, the relaxation changes scale quadratically with the radius of the droplet, while for fixed droplet size the relaxation changes will scale linearly with the oil volume fraction. At constant f and radius R, the relaxation varies quadratically with $\Delta\chi$.

MATERIALS AND METHODS

$\Delta\chi$ Measurements

The susceptibility of olive oil could not be found in the literature. Therefore, the difference in magnetic susceptibility ($\Delta\chi$) between olive oil and water was measured according to the imaging-based method proposed by Weisskoff and Kiihne (20). A spherical glass phantom (diameter 16 cm) with a cylindrical nylon inset (diameter 1.6 cm) was built as shown in Fig. 1a. The phantom was placed in the center of the scanner bore with the cylinder perpendicular to the main B_0 field. The phantom was filled with water and the nylon cylindrical inset was filled alternately with water or olive oil. Coronal phase maps were acquired at different echo times. The water phase maps were then subtracted from the oil phase maps, and the phase variation induced by the oil was measured.

The variation in phase ($\Delta\phi$) induced in the surrounding water, in a direction along the B_0 field, by the oil in the inner cylinder can be expressed as (20)

$$\Delta\phi = \frac{\gamma B_0 \Delta\chi}{2} \left(\frac{R}{r}\right)^2 \tau,$$
[2]

where R is the radius of the inner cilinder, γ the proton gyromagnetic ratio, τ the echo time used in the imaging module, r the distance from the center of the cylinder, and $\Delta\chi$ the susceptibility difference expressed in SI units. Fitting the signal intensity profile along the main field B_0 (shown in Fig. 1b) of the subtracted phase maps will therefore yield $\Delta\chi$ (the value of $\Delta\chi$ in cgs units is obtained by dividing by 4π).
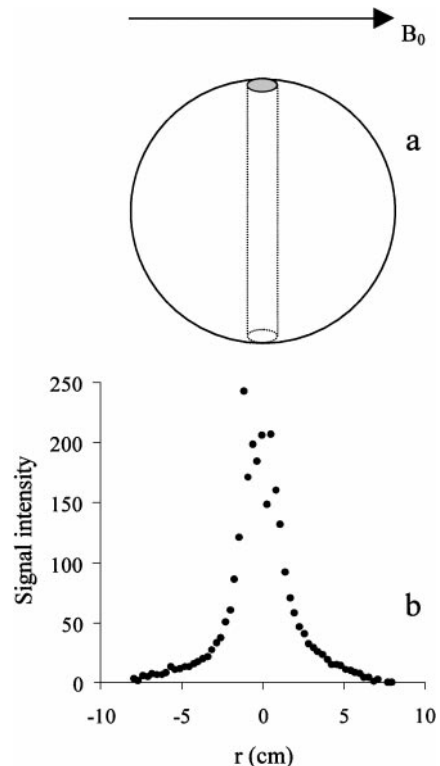

FIG. 1. (a) Schematic diagram of the glass spherical phantom used to measure the difference in susceptibility $\Delta\chi$ between olive oil and water. The phantom was filled with water and the nylon cylindrical insert (perpendicular to the main B_0 field) was alternatively filled with water or olive oil. Coronal phase maps were acquired at different echo times. The control water phase maps were then subtracted from the oil maps and the phase variation induced by the oil along the B_0 field measured. (b) An example of the signal intensity variation along B_0 versus the distance r from the center of the oil inset in a subtracted phase image.

Oil-in-Water Emulsion Preparation

A range of simple food grade oil-in-water emulsions were produced using 8% w/w olive oil (low saturates, Sainsburys, UK) and 2% w/w monostearate emulsifier (Crillet3, Croda food, Lancashire, UK). These emulsions were prepared as concentrated premixes (15% w/w olive oil, stabilized with 0.1–0.2% w/w surfactant), using a BL300T Kenwood blender (Kenwood, Surrey, UK) (30–60 s bursts), and then diluted to the required concentrations with a continuous phase containing the remaining surfactant. By varying the fraction of the total surfactant used in the production of the premix, time and intensity of homogenization, and temperature (between 1°C and room temperature) of the two phases prior to homogenization, emulsions of differing droplet diameters (between 0.6 and 20 μm) were produced.

A second set of oil-in water emulsions was produced using 20% w/w olive oil and sorbitan monooleate emulsifier (Span 80, SIGMA). These emulsions were prepared using a PB20E Waring blender (Waring, Torrington, CT, USA). The emulsifier was first dissolved in oil (15 s burst). Secondly, this premix was diluted with water to the required concentration and homogenized

(180 s burst). Emulsions of differing droplet diameters were produced by varying the surfactant concentration from 1.5 (for the large 12-μm emulsion) to 5% w/w (for the small 3-μm emulsion).

A Coulter LS230 light diffraction sizer (Beckman Coulter, Buckinghamshire, UK) was used to determine the weight mean droplet diameter. Droplet size distributions were calculated using a standard olive oil optical model (Fluid R.I. 1.333; Sample R.I. Real 1.456, Imag. 0.01).

Monte Carlo Simulations

Proton random walk simulations were performed to model the signal changes due to the diffusion of water protons through spatially varying fields, produced by the difference in susceptibility between oil and water. The simulation procedure used has been detailed previously (*11*). In particular, steps that resulted in the water proton moving inside the oil droplet were rejected. The pseudorandom number generator used was the Mersenne Twister, which has a period of $2^{19,937}-1$ and excellent equidistribution properties (*21*). The uniform distribution was converted to a normal distribution using the Box–Muller method outlined in "Numerical Recipes in C" (*22*). Simulations were performed with 20,000 protons. The phase of each proton was accumulated as it performed a random walk through a space containing the oil droplets. The diameter of the oil droplets was varied from 4 to 50 μm at a constant oil volume fraction of 8%. The random walk was performed to a time of 100 ms and the phase history of each proton was stored at 5-ms intervals. The temporal sampling interval used was 43 μs, corresponding to a proton displacement of 0.5 μm for $D = 2.9 \times 10^{-9}$ m^2/s, the estimated value for water at 37°C. At a field of 0.5 T the frequency shift on the surface of the oil droplets is small (1 ppm corresponds to a 22-Hz shift, and a maximum phase accumulation of 0.94×10^{-3} radians in one time step), ensuring adequate sampling.

Magnetic Resonance Imaging

MRI was performed on a whole-body 0.5-T purpose-built EPI scanner equipped with actively shielded gradient coils. A 50-cm diameter bird-cage coil was used to acquire single-shot MBEST EPI (*23, 24*) images in 130 ms, with a slice thickness of 1 cm, using a 128×128 matrix with 3.5×2.5 mm^2 in-plane resolution. T_1 data was acquired using an inversion recovery EPI sequence at 15 different inversion times varying from 60 ms to 12 s, with a hyperbolic secant inversion pulse. T_2 data were acquired using a spin-echo EPI sequence at eight echo times varying from 60 to 700 ms.

The measurements were carried out at 37°C on five different 8% oil-in-water monostearate emulsions and six different 20% oil-in-water sorbitan monooleate emulsions with varying droplet size. Finally, in order to confirm the observed effect of $\Delta \chi$ on the transverse relaxation rate, five batches of the 12-μm, 8% oil-in-water monostearate emulsion were prepared. The water phase

of each batch was doped with Gadoteridol (ProHance, Bracco) increasing from 0 to 0.6 mM and T_2 was measured at 37°C. Similar measurements were made for the water phase alone with increasing doping in order to calculate the experimental ΔR_2.

RESULTS

Figure 2 shows two examples of the droplet size distributions obtained from the laser diffraction measurements. The mean emulsion droplet diameters produced were 0.4, 2.7, 6.4, 11.6, and 20.9 μm for the 8% oil-in-water monostearate emulsion and 3.2, 4.1, 5.2, 6.5, 7.8, and 12 μm for the 20% oil-in-water sorbitan monooleate emulsion. The largest droplet emulsion for each series of emulsions was observed to cream over the course of the experiment, that is to say, a fat layer was observed on the surface of the beaker. The magnetic susceptibility difference between olive oil and water was measured to be $\Delta \chi = 1.55$ ppm (1.23×10^{-7} cgs units). This corresponds to an equatorial frequency shift, $\delta \omega$, of 5.5 rad/s on the surface of the oil droplet at 0.5 T. For a diffusion coefficient of 2.9×10^{-9} m^2/s, the analytical expression in Eq. [1] above will be valid for droplet diameters less than about 12 μm. When the water phase was doped with 0.4 mM Gadoteridol this fell to $\Delta \chi = 0.96$ ppm, indicating that oil has a positive susceptibility.

No trends in T_1 with changing emulsion droplet size were found for the 8% oil emulsion (mean $T_1 = 2.86$ s). However it was observed that the transverse relaxation rate $1/T_2$ increased
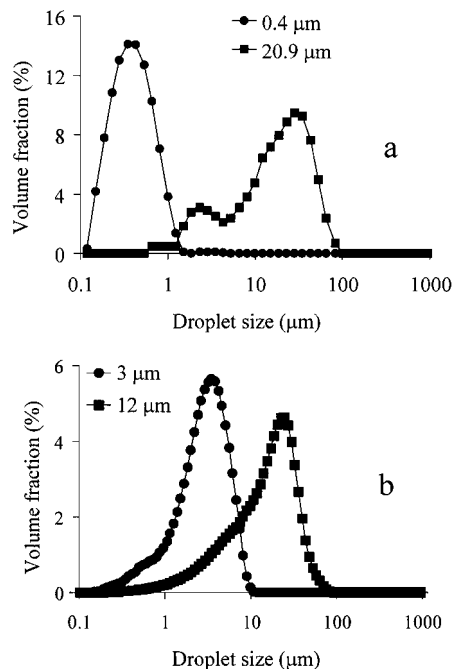

FIG. 2. Examples of laser diffraction measurements of the droplet diameter distributions. The smallest and largest oil droplet distributions for (a) the 8% and (b) the 20% oil-in-water emulsions used in this study are shown.

for larger droplet sizes as shown in Fig. 3a. The figure also shows the plot of the analytical expression given in Eq. [1] (with T_2 for the water phase measured to be 2 s), and the results of the Monte Carlo random walk simulation performed using the measured value of $\Delta\chi$. Figure 3b shows the experimental data acquired on the 20% oil emulsion and the plot of the analytical expression given in Eq. [1] (with T_2 for the water phase fitted to 1.67 s). As predicted, the dependence of $1/T_2$ on droplet size is quadratic (correlation coefficient $R^2 = 0.99$) when the data from the larger samples (12 μm), which were creaming during the experiment, are excluded from the fit.

Figure 4 shows the variation of the measured ΔR_2 as the $\Delta\chi$ between the water and oil phases of the fixed 12-μm (8% oil)

FIG. 4. Variation of $\Delta R_2 = (1/T_2)_{\text{observed}} - (1/T_2)_{\text{water}}$ with increasing difference in magnetic susceptibility $\Delta\chi$ between the oil and the water phases of a 12-μm diameter 8% oil-in-water emulsion at 37°C. $\Delta\chi$ was varied by progressively doping the water phase of different emulsion batches with gadolinium ($n = 1$ for each gadolinium concentration). The solid circles represent the experimental data, and the dotted line shows the analytical expression calculated from Eq. [1] (correlation coefficient $R^2 = 0.96$).
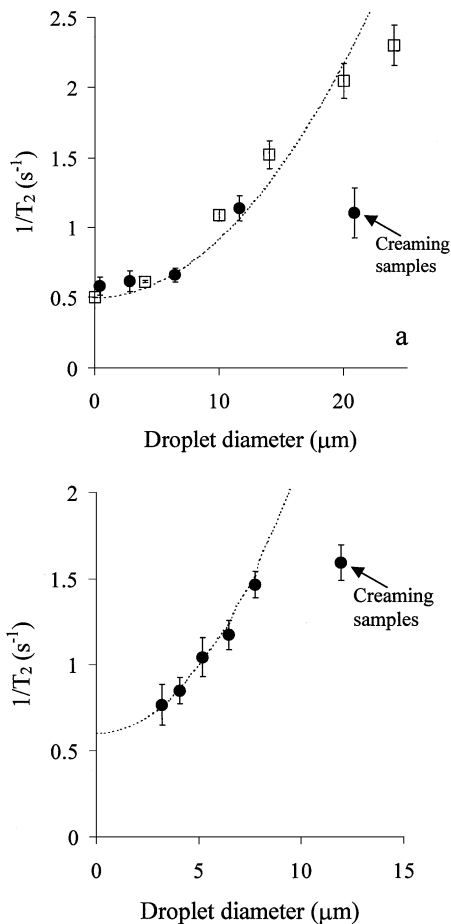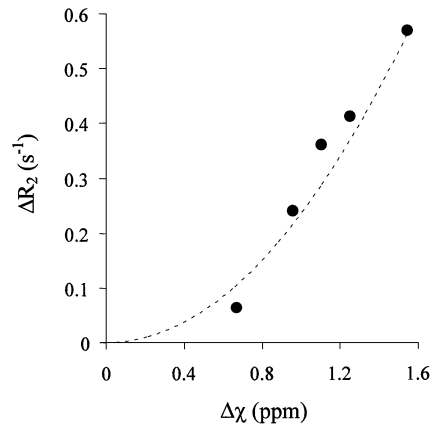

FIG. 3. Plot of oil-in-water emulsion $1/T_2$ (mean ± SD) versus oil droplet mean size. (a) shows the data for the 8% oil-in-water monostearate emulsion. The solid circles represent the experimental data, the open squares the Monte Carlo simulation results, and the dotted line is the analytical expression given in Eq. [1]. The arrow indicates the largest (20.9 μm) emulsion, which was unstable and showed visible creaming during the course of the experiment. Creaming lowers the oil fraction in solution and thus the $1/T_2$. (b) shows the data for the 20% oil-in-water sorbitan monooleate emulsion. The solid circles represent the experimental data and the dotted line is the analytical expression given in Eq. [1]. The fit calculated excluding the largest (arrow, 12 μm) emulsion, which showed creaming, had a correlation coefficient $R^2 = 0.99$.

emulsions was reduced by doping the water phase with Gadoteridol. As predicted by Eq. [1] (plotted as a dotted line on Fig. 4), the dependence of ΔR_2 on $\Delta\chi$ is quadratic (correlation coefficient $R^2 = 0.96$).

DISCUSSION

Good agreement was found between the transverse relaxation rates measured for both series of emulsions and the analytical expression in the motionally narrowed regime. Good agreement was also found between the Monte Carlo random walk simulations and the data for the 8% oil-in-water monostearate emulsions. The increased oil fraction of the 20% oil emulsion showed increased sensitivity to changes in droplet size as predicted by Eq. [1]. In both cases the signal from the oil was neglected because the T_2 of oil (approx 70 ms) is much less than that of water, and will have largely decayed by the center of k-space for the EPI acquisition (the fat signal is also shifted by the high bandwidth per pixel). In both emulsion systems we were unable to prepare stable emulsions at larger sizes using the current preparation methods. They showed visible creaming during the course of the experiment. The buoyancy of large droplets forces them to layer on the top of the beaker, lowering the oil fraction in solution and hence, as expected, the experimental $1/T_2$. It was not possible to investigate the effect of the variation of emulsifier concentration (1.5–5%) in the 20% oil emulsion system on $1/T_2$ as the Span 80 is poorly soluble in water alone. However, the fit to Fig. 3b indicates that the emulsifier shortens T_2 for the water phase slightly. Therefore, the increasing concentration of emulsifier with smaller droplet diameter would be expected to reduce the gradient of Fig. 3b with respect to the analytical expression. There is a slight trend for this to be

observed, but the effect is small. The experiments with the 8% oil emulsions were conducted with a fixed fraction of emulsifier in solution.

The data indicate that the droplet size sensitivity of T_2 is due to the diffusion of water protons in the microscopic gradients created at the interface of the oil and water due to the magnetic susceptibility difference between them. The experiment that involved doping of the water phase of a given emulsion with gadolinium (hence modifying $\Delta\chi$) supported this explanation. The range of droplet size considered is of biological interest but, if necessary, the sensitivity of the technique could be increased by appropriately doping the water or the oil phase of the emulsions to increase the susceptibility difference. A similar approach could be used to extend it to different emulsion systems. T_1 did not vary significantly with droplet size as surface relaxation is not expected to be a major contribution in T_1 relaxation of oil emulsions (14). It should also be noted that the quadratic dependence of $1/T_2$ on droplet size will weight the larger droplets in the distribution more, but given the width of the distributions and their natural tendency to be skewed toward smaller diameters this will usually not be relevant. It is also important to note that the T_2 dependence on droplet size should be considered when using multicomponent T_1 data to assess emulsions fat fraction.

The measurement of fat emulsification in the gastric lumen is important, as the rate of absorption and subsequent metabolism of fat depends critically on the available surface area, and hence on emulsion particle size. T_2 measurements have the potential to provide a robust method of assessing emulsion droplet *in vivo*. We have previously shown that EPI can overcome gastrointestinal motion, and allow quantitative transverse relaxation measurements in reasonable times (25). It should be noted, however, that there may be other factors that will alter the emulsion transverse relaxation *in vivo*. Fat concentration in the gastric lumen will change with time due to meal dilution by secretion, emptying, and layering. Therefore it would be necessary to simultaneously determine the fat concentration at each time point, which could be achieved using techniques such as direct water/fat suppressed imaging, fat/water localized spectroscopy or T_1 measurements (12–14). The spin-echo EPI T_2 measurements would then allow the quantitative measurement of particle size of emulsified oil in the gastric lumen throughout digestion.

CONCLUSIONS

This paper introduces a novel method of measuring fat emulsion size using the dependence of transverse relaxation on oil droplet size. This method could potentially be used *in vivo* in the gastric lumen. This would make it possible to extend the MRI investigations of the gastrointestinal system to the study of the effects of gastric motor function on fat emulsification. The emulsions used in this work are food-grade, acceptable to volunteers, and provide good contrast between the gastric lumen

and the surrounding organs. Further work is underway to investigate the feasibility of using this method *in vivo* against laser diffraction measurements on naso-gastric aspirates and to further validate the method by comparing the results of single-echo and multiecho T_2 measurements.

REFERENCES

1. C. E. Bohren and D. R. Huffman, "Absorption and Scattering of Light by Small Particles," Wiley, New York (1983).

2. K. J. Packer and C. J. Rees, Pulsed NMR studies of restricted diffusion, *J. Colloid Interface Sci.* **40,** 206–218 (1972).

3. J. C. Van Den Enden, D. Waddington, H. Van Aalst, C. G. Van Kralingen, and K. J. Packer, Rapid determination of water droplet size distributions by PFG-NMR, *J. Colloid Interface Sci.* **140,** 105–113 (1990).

4. I. Lönnqvist, A. Kahn, and O. Söderman, Characterization of emulsions by NMR methods, *J. Colloid Interface Sci.* **144,** 401–411 (1991).

5. I. Lönnqvist, B. Hakansson, B. Balinov, and O. Söderman, NMR self-diffusion studies of the water and the oil components in a W/O/W emulsion, *J. Colloid Interface Sci.* **192,** 66–73 (1997).

6. H. Wennerström, Macroemulsions versus microemulsions, *Colloid Surf. A: Phys. Eng. Aspect* **123,** 13–26 (1997).

7. L. Ambrosone, A. Ceglie, G. Colafemmina, and G. Palazzo, General methods for determining the droplet size distribution in emulsion systems, *J. Chem. Phys.* **110,** 797–804 (1999).

8. B. Håkansson, R. Pons, and O. Söderman, Diffraction-like effects in a highly concentrated W/O emulsion: a PFG NMR study, *Magn. Reson. Imaging* **16,** 643–646 (1998).

9. R. N. Muller, P. Gillis, F. Moiny, and A. Roch, Transverse relaxivity of particulate MRI contrast media: From theories to experiments, *Magn. Reson. Med.* **22,** 178–182 (1991).

10. R. P. Kennan, J. Zhong, and J. C. Gore, Intravascular susceptibility contrast mechanisms in tissues, *Magn. Reson. Med.* **31,** 9–21 (1994).

11. R. M. Weiskoff, C. S. Zuo, J. L. Boxerman, and B. R. Rosen, Microscopic susceptibility variation and transverse relaxation: theory and experiment, *Magn. Reson. Med.* **31,** 601–610 (1994).

12. R. J. Kauten, J. E. Maneval, and M. J. McCarthy, Fast determination of spatially localized volume fractions in emulsions, *J. Food Sci.* **56,** 799–801 (1991).

13. B. P. Hills, P. Manoj, and C. Destruel, NMR Q-space microscopy of concentrated oil-in-water emulsions, *Magn. Reson. Imaging* **18,** 319–333 (2000).

14. P. J. McDonald, E. Ciampi, J. L. Keddie, M. Heidenreich, and R. Kimmich, Magnetic resonance determination of the spatial dependence of the droplet size distribution in the cream layer of oil-in-water emulsions: evidence for the effect of depletion flocculation, *Phys. Rev. E* **59,** 874–884 (1999).

15. V. G. Kiselev and S. Posse, Analytical theory of susceptibility induced NMR signal dephasing in a cerebrovascular network, *Phys. Rev. Lett.* **81,** 5696–5699 (1998).

16. K. J. Packer, The effects of diffusion through locally inhomogeneous magnetic fields on transverse nuclear spin relaxation in heterogeneous systems. Proton transverse relaxation in striated muscle tissue, *J. Magn. Reson.* **9,** 438–443 (1973).

17. P. Gillis and S. H. Koenig, Transverse relaxation of solvent protons induced by magnetized spheres: application to ferritin, erythrocytes, and magnetite, *Magn. Reson. Med.* **5,** 323–345 (1987).

18. J. H. Freed, Dynamic effects of pair correlation functions on spin relaxation by translational diffusion in liquids. II. Finite jumps and independent T_1 processes, *J. Chem. Phys.,* **68,** 4034–4037 (1978).

19. D. A. Yablonskiy and E. M. Haacke, Theory of NMR signal behaviour in magnetically inhomogeneous tissues: The static dephasing regime, *Magn. Reson. Med.* **32,** 749–763 (1994).

20. R. M. Weisskoff and S. Kiihne, MRI Susceptometry: image based measurement of absolute susceptibility of MR contrast agents and human blood, *Magn. Reson. Med.* **24,** 375–383 (1992).

21. M. Matsumoto and T. Nishimura, Mersenne Twister: A 623-dimensionally equidistributed uniform pseudorandom number generator, *ACM Trans. Model. Comput. Simul.* **8,** 3–30 (1998).

22. W. H. Press, S. A. Teukolsky, W. T. Vetterling, and B. P. Flannery, "Numerical Recipes in C: The Art of Scientific Computing," 2nd ed., Cambridge Univ. Press, Cambridge, UK (1992).

23. P. Mansfield, Multi-planar image formation using NMR spin echoes, *J. Phys.* **10,** L55–L58 (1977).

24. A. M. Howseman, M. K. Stehling, B. Chapman, R. Coxon, L. Turner, R. J. Ordidge, M. G. Cawley, P. Glover, P. Mansfield, and R. E. Coupland, Improvements in snap-shot nuclear magnetic resonance imaging, *Br. J. Radiol.* **61,** 822–828 (1988).

25. L. Marciani, P. A. Gowland, R. C. Spiller, P. Manoj, R. J. Moore, P. Young, and A. Fillery-Travis, Effect of meal viscosity and nutrients on satiety, intragastric dilution and emptying assessed by MRI, *Am. J. Physiol.* **280,** G1227–G1233 (2001).